

phys. stat. sol. (b) **189**, 193 (1995)

Subject classification: 72.10 and 73.40; S7.12; S7.15

*Department of Physics and Meteorology, Indian Institute of Technology, Kharagpur<sup>1</sup>) (a) and Departamento de Física de Materiales, Facultad de Físicas, Universidad Complutense, Madrid<sup>2</sup>) (b)*

## Temperature Dependence of Conductance of Fibonacci Superlattices

By

C. L. ROY (a), CHANDAN BASU (a), F. DOMÍNGUEZ-ADAME (b), and E. MACIÁ (b)

Studies of the dc conductance of Fibonacci superlattices at finite temperature are carried out. Exact solutions of the Schrödinger equation are used for our treatment of the problem. The results show a strong dependence of electrical conduction on the chemical potential, which acts as a probe of the underlying electronic structure. In particular, it is found that the Fibonacci superlattice shows metallic behaviour when the chemical potential lies within allowed bands and it behaves as a semiconductor when the chemical potential lies within gaps.

### 1. Introduction

It is well established that electron localization in intentionally disordered quantum-well based GaAs–Ga<sub>1-x</sub>Al<sub>x</sub>As superlattices are due to the loss of quantum coherence [1]. Further, a number of studies have been performed on carrier dynamics in superlattices with uncorrelated [2 to 4] and correlated [5 to 7] disorder. Besides intentionally disordered superlattices, it has been possible to grow quasiperiodic quantum-well superlattices [8]. Most researches have considered Fibonacci superlattices (FSLs) as the archetype of quasiperiodic heterostructures. One of the most conspicuous features of electron dynamics in these systems is the occurrence of a highly fragmented, self-similar electronic spectrum with a hierarchy of splitting subbands [9 to 11]. This rather exotic electronic spectrum strongly influences electron propagation [12, 13] and Landauer resistance of the FSL [14]. Using a tight-binding model for the FSL, Maciá et al. [15] have previously investigated the influence of the underlying spectrum structure on the dc conductance at different temperatures. The aim of this paper is to extend further these treatments considering a more elaborated model within the effective-mass approximation.

### 2. Model

We describe electron dynamics by a scalar Hamiltonian corresponding to decoupled bands in the host semiconductors. The corresponding wave equation for the envelope function is a Schrödinger-like equation for a particle of an energy-independent effective mass  $m^*$ , assumed to be constant throughout the FSL. Isotropic and parabolic bands usually work well in some III–V compounds near the band edge. In particular, our results are valid in the most widely investigated superlattice, namely GaAs–Ga<sub>1-x</sub>Al<sub>x</sub>As. In order to grow a

<sup>1</sup>) Kharagpur 721 302, India.

<sup>2</sup>) E-28040 Madrid, Spain.

FSL, we have to define two distinct building blocks, say A and B, and to arrange them according to the Fibonacci sequence. Each building block can be composed of one or more layers of different materials and can have arbitrary thickness. A Fibonacci sequence  $\{S_n\}$  of order  $n$  is obtained by  $n$  successive applications of the substitution rule  $A \rightarrow AB$  and  $B \rightarrow A$ . The obtained sequence comprises  $F_{n-1}$  elements A and  $F_{n-2}$  elements B,  $F_n$  being a Fibonacci number obtained from the recurrent law  $F_n = F_{n-1} + F_{n-2}$  with  $F_0 = F_1 = 1$ . For our treatment, we have taken rectangular potential barriers, due to conduction-band offsets at the interfaces in GaAs–Ga<sub>1-x</sub>Al<sub>x</sub>As, to obtain the FSL. Hence we are neglecting band bending at the interfaces of the FSL. The dynamics of electrons in this superlattice can be described by the following equation:

$$\left[ -\frac{1}{2} \frac{d^2}{dz^2} + \sum_{i=1}^N V(z - z_i) \right] \Psi(z) = E\Psi(z), \quad (1)$$

in units such that  $\hbar = m^* = 1$ ; these units set the energy and length scales to be 11 meV and 5 nm in GaAs, respectively. The superlattice potential is  $V(z - z_i) = V_i$  for  $|z - z_i| \leq b_i/2$  and vanishes otherwise. Here  $V_i$  and  $b_i$  are the heights and widths of the rectangular potential barriers. These parameters take on the values  $V_i = V_A$  or  $V_B$  and  $b_i = b_A$  or  $b_B$  according to the Fibonacci sequence. Assuming non-overlapping potentials, as usual in semiconductor superlattices, (1) can be solved piecewise exactly using the well-known transfer matrix formalism [14]. In particular, this method allows us to find the transmission coefficient  $\tau(E)$  for any incident electron energy  $E$ . Therefore, using the Landauer formula [16] it is possible to obtain the dc conductance at zero temperature  $\kappa_0(E)$  in units of  $e^2/h$  as follows:

$$\kappa_0(E) = \frac{\tau(E)}{1 - \tau(E)}. \quad (2)$$

To compute the dc conductance of the system at finite temperature  $\kappa(T, \mu)$  we take recourse to the following expression due to Engquist and Anderson [17]:

$$\kappa(T, \mu) = \frac{\int \left( -\frac{\partial f}{\partial E} \right) \tau(E) dE}{\int \left( -\frac{\partial f}{\partial E} \right) [1 - \tau(E)] dE}, \quad (3)$$

where  $f$  is the Fermi-Dirac distribution and  $\mu$  the chemical potential. Then, we have  $\lim_{T \rightarrow 0} \kappa(T, \mu) = \kappa_0(E = \mu)$ , that is, at zero temperature only electrons at the Fermi level contribute to electronic conduction.

### 3. Results and Discussion

The main emphasis of our numerical analysis is to evaluate  $\kappa(T, \mu)$  over a wide range of temperatures (from 0 up to about 1000 K). For our calculations we have chosen a FSL of order  $n = 15$  so that the total number of barriers is  $N = F_{15} = 987$ . The separation between nearest barriers is fixed at 2.5 (12.5 nm). Moreover, the conduction-band offset we consider corresponds to heterojunctions GaAs–Ga<sub>1-x</sub>Al<sub>x</sub>As with  $x \approx 0.5$ , i.e. barrier heights of order of 55 meV. First of all, we have studied the conductance of the sample at zero temperature, i.e.,  $\kappa_0(E)$ , as a function of the electron energy. The results are shown in Fig. 1,

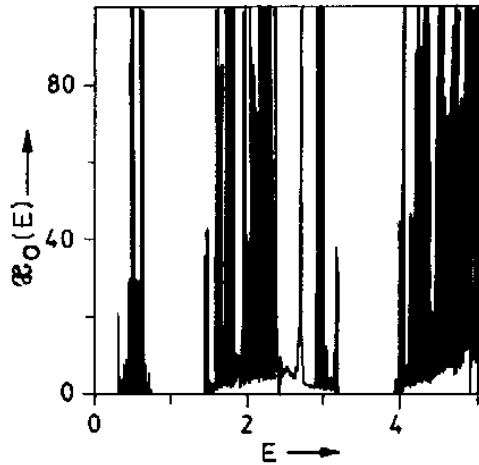


Fig. 1. Dc conductance at zero temperature as a function of the electron energy for  $V_A = 5.0$ ,  $V_B = 4.95$  and  $b_A = b_B = 0.2$

where it is noticeable that the highly fragmented nature of the spectrum causes strong fluctuations of the value in the conductance, even for minor deviations from periodicity (the ratio  $V_A/V_B$  is very close to unity). This feature can be understood [18] from the fact that, for any finite approximation of the FSL, the allowed energies form a set of sparse points approximating a pre-fractal Cantor-set structure. As the electron energy equals one of these energy levels, an enhanced resonant tunnelling takes place, leading to high conductance peaks. In other words, the regions where  $\kappa_0(E)$  is large are allowed regions of energies.

The results for dc conductance at finite temperature are shown in Fig. 2, where each unit of  $kT$  ( $k$  is the Boltzmann constant) corresponds to  $T \approx 130$  K. The shape of these curves show strong dependence of  $\kappa(T, \mu)$  on the value of the chemical potential  $\mu$ . Hence, we have considered two different cases. In the first one, we assume that the Fermi level lies within an allowed band. In this case, which is elaborated by graphs 1 and 2 of Fig. 2, the curves  $\kappa(T, \mu)$  show hump-like behaviour at low temperatures, similar to what is reported in [15]. At higher temperatures,  $\kappa(T, \mu)$  decreases with  $T$  and reaches an asymptotic value on further increasing  $T$ . The high values of dc conductance as well as their dependence on  $T$  are similar to those metals whose Fermi energy is located within the conduction band. In the second case, we study the behaviour of  $\kappa(T, \mu)$  when the Fermi level falls within a forbidden

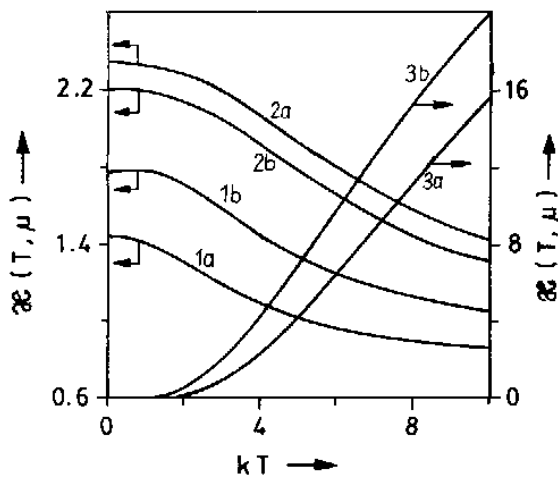


Fig. 2. Dc conductance as a function of temperature for three different values of the chemical potential; (1)  $\mu = 4.0$ , (2)  $3.0$ , and (3)  $3.8$ . Curves labeled a correspond to the same barrier parameters as in Fig. 1, whereas curves labeled b correspond to the  $\delta$ -function limit of the barriers (zero width and constant area  $\lambda$ ) with strengths  $\lambda_A = 1.00$  and  $\lambda_B = 0.99$

region. This situation is demonstrated by curves 3 in Fig. 2. Here, dc conductance is very small initially and increases monotonically with temperature, although the numerical values are one order of magnitude smaller than in the previous case. This behaviour is like that of semiconductors whose Fermi level falls within the gap. Moreover, from Fig. 2 we see that the behaviour of  $\kappa(T, \mu)$  is qualitatively the same for barrier potentials and  $\delta$ -function potentials, although the results differ noticeably from the quantitative viewpoint.

#### 4. Conclusions

We have studied a semiconductor superlattice in which the constituent blocks are arranged according to the Fibonacci sequence. We have used exact solutions of the Schrödinger-like equation for the electronic envelope functions in the effective mass framework. The energy spectrum shows the typical features of quasiperiodic systems: The spectrum appears highly fragmented and displays a well-developed self-similar structure, characteristic of a pre-fractal Cantor-like set. The electronic structure of the energy spectrum is naturally translated into the dc conductance of such system. The dc conductance shows metallic or semiconductor behaviour, depending on whether the chemical potential lies within or outside an allowed band, respectively. Hence the chemical potential may be used as a probe of the electronic spectrum. The way to scan the chemical potential over the spectrum is achieved by changing pressure, doping, or the applied voltage at the buffer layers. This shows the possibility of a certain degree of engineering on transport properties during sample growth, by adjusting chemical composition and sample length suitably. This result can be of significant importance in view of growing applications of superlattice structures.

#### Acknowledgements

Chandan Basu is grateful to CSIR, India, for providing him financial support. Work at Madrid is supported by UCM under project PR161/93-4811.

#### References

- [1] A. CHAMOTTE, B. DEVEAUD, A. REGRENY, and G. BASTARD, Phys. Rev. Letters **57**, 1064 (1986).
- [2] A. SASAKI, M. KASU, T. YAMAMOTO, and S. NODA, Japan. J. appl. Phys. **28**, L1249 (1989).
- [3] M. KASU, T. YAMAMOTO, S. NODA, and A. SASAKI, Appl. Phys. Letters **59**, 800 (1991).
- [4] X. CHEN and S. XIONG, Phys. Rev. B **47**, 7146 (1993).
- [5] A. SÁNCHEZ, E. MACIÁ, and F. DOMÍNGUEZ-ADAME, Phys. Rev. B **49**, 147 (1994).
- [6] E. DIEZ, A. SÁNCHEZ, and F. DOMÍNGUEZ-ADAME, Phys. Rev. B **50**, 14359 (1994).
- [7] F. DOMÍNGUEZ-ADAME, A. SÁNCHEZ, and E. DIEZ, Phys. Rev. B **50**, R17736 (1994).
- [8] R. MERLIN, K. BAJEMA, R. CLARKE, F.-Y. JUANG, and P. K. BHATACHARYA, Phys. Rev. Letters **55**, 1768 (1985).
- [9] F. LARUELLE and B. ETIENNE, Phys. Rev. B **37**, 4816 (1988).
- [10] E. MACIÁ, F. DOMÍNGUEZ-ADAME, and A. SÁNCHEZ, Phys. Rev. E **50**, R679 (1994).
- [11] F. DOMÍNGUEZ-ADAME, E. MACIÁ, and B. MÉNDEZ, Phys. Letters A **194**, 184 (1994).
- [12] S. KATSUMOTO, N. SANO, and S. KOBAYASHI, Solid State Commun. **85**, 223 (1993).
- [13] F. DOMÍNGUEZ-ADAME and A. SÁNCHEZ, Phys. Letters A **159**, 153 (1991).
- [14] C. L. ROY and ARIF KHAN, Phys. Rev. B **49**, 14979 (1994).
- [15] E. MACIÁ, F. DOMÍNGUEZ-ADAME, and A. SÁNCHEZ, Phys. Rev. B **49**, 9503 (1994).
- [16] R. LANDAUER, IBM J. Res. Developm. **1**, 223 (1957).
- [17] H. L. ENGQUIST and P. W. ANDERSON, Phys. Rev. B **24**, 1151 (1981).
- [18] S. DAS SARMA and X. C. XIE, Phys. Rev. B **37**, 1097 (1988).

(Received November 8, 1994)